

Structural variations of the first family of heterometallic uranyl carboxyphosphinate assemblies by synergy between carboxyphosphinate and imidazole ligands

Weiting Yang,^a Dai Wu,^a Chao Liu,^a Qing-Jiang Pan^{*b}, and Zhong-Ming Sun^{*a}

^aState Key Laboratory of Rare Earth Resource Utilization, Changchun Institute of Applied Chemistry, Chinese Academy of Sciences, 5625 Renmin Street, Changchun, Jilin 130022, China.

^bKey Laboratory of Functional Inorganic Material Chemistry of Education Ministry, School of Chemistry and Materials Science, Heilongjiang University, Harbin 150080, China.

SUPPORTING INFORMATION

I. Tables.

Table S1 Selected bond lengths and angles for **1-8**.

Table S2 Average bond lengths of six-fold and seven-fold coordinated uranium cations in **1-8**.

Table S3 IR spectroscopic data for **1-8**.

Table S4 Comparison of selected single-crystal XRD and IR spectroscopic data for **1-8** using Veal's empirical law.

II. Powder X-ray diffraction patterns.

Figure S1. PXRD pattern of Co(im)₂(UO₂)₃(L)₄ **1**.

Figure S2. PXRD pattern of Zn(bpi)(UO₂)(L)₂ **2**.

Figure S3. PXRD pattern of Mn(dib)(UO₂)₂(L)₃ **5**.

Figure S4. PXRD pattern of [Co(dib)₂(H₂O)₂][(UO₂)₃(L)₄]·2H₂O **6**.

Figure S5. PXRD pattern of [Ni(dib)₂(H₂O)₂][(UO₂)₃(L)₄]·2H₂O **7**.

III. Infrared spectra

Figure S6. IR spectrum of Co(im)₂(UO₂)₃(L)₄ **1**.

Figure S7. IR spectrum of Zn(bpi)(UO₂)(L)₂ **2**.

Figure S8. IR spectrum of Cd(dib)(UO₂)(L)₂ **3**.

Figure S9. IR spectrum of Cd(dib)(UO₂)₂(L)₃ **4**.

Figure S10. IR spectrum of Mn(dib)(UO₂)₂(L)₃ **5**.

Figure S11. IR spectrum of [Co(dib)₂(H₂O)₂][(UO₂)₃(L)₄]·2H₂O **6**.

Figure S12. IR spectrum of $[\text{Ni}(\text{dib})_2(\text{H}_2\text{O})_2][(\text{UO}_2)_3(\text{L})_4]\cdot 2\text{H}_2\text{O}$ **7**.

Figure S13. IR spectrum of $[\text{Cu}(\text{dib})_2(\text{H}_2\text{O})_2][(\text{UO}_2)_3(\text{L})_4]$ **8**.

IV. ORTEP representation of local structures.

Figure S14. ORTEP representation of local structure of $\text{Co}(\text{im})_2(\text{UO}_2)_3(\text{L})_4$ **1**.

Figure S15. ORTEP representation of local structure of $\text{Zn}(\text{bpi})(\text{UO}_2)(\text{L})_2$ **2**.

Figure S16. ORTEP representation of local structure of $\text{Cd}(\text{dib})(\text{UO}_2)(\text{L})_2$ **3**.

Figure S17. ORTEP representation of local structure of $\text{Mn}(\text{dib})(\text{UO}_2)_2(\text{L})_3$ **5**.

Figure S18. ORTEP representation of local structure of $[\text{Co}(\text{dib})_2(\text{H}_2\text{O})_2][(\text{UO}_2)_3(\text{L})_4]\cdot 2\text{H}_2\text{O}$ **6**.

V.Excitation and Emission spectra.

Figure S19. Excitation and emission spectra of $\text{Co}(\text{im})_2(\text{UO}_2)_3(\text{L})_4$ **1**.

Figure S20. Excitation and emission spectra of $\text{Mn}(\text{dib})(\text{UO}_2)_2(\text{L})_3$ **5**.

Figure S21. Excitation and emission spectra of $[\text{Co}(\text{dib})_2(\text{H}_2\text{O})_2][(\text{UO}_2)_3(\text{L})_4]\cdot 2\text{H}_2\text{O}$ **6**.

Figure S22. Excitation and emission spectra of $[\text{Ni}(\text{dib})_2(\text{H}_2\text{O})_2][(\text{UO}_2)_3(\text{L})_4]\cdot 2\text{H}_2\text{O}$ **7**.

Figure S23. Excitation and emission spectra of the carboxphosphinate ligand **CPP**.

Figure S24. Excitation and emission spectra of imidazole.

Figure S25. Excitation and emission spectra of **bpi**.

Figure S26. Excitation and emission spectra of **dib**.

I. Tables.

Table S1 Selected bond lengths (\AA) and angles ($^\circ$) for **1-8**.

1			
U(1)-O(1)#1	1.729(9)	U(2)-O(3)	1.695(9)
U(1)-O(1)	1.729(9)	U(2)-O(2)	1.733(8)
U(1)-O(5)	2.283(9)	U(2)-O(11)#3	2.290(8)
U(1)-O(5)#1	2.283(9)	U(2)-O(4)	2.301(9)
U(1)-O(10)#2	2.299(8)	U(2)-O(6)#4	2.305(9)
U(1)-O(10)#3	2.299(8)	U(2)-O(9)	2.465(9)
		U(2)-O(8)	2.549(9)
Co(1)-O(7)#4	2.078(8)	P(1)-O(4)	1.507(9)
Co(1)-O(7)#5	2.078(8)	P(1)-O(5)	1.516(9)
Co(1)-N(1)#6	2.124(12)	P(1)-C(7)	1.759(13)
Co(1)-N(1)	2.124(12)	P(1)-C(1)	1.779(14)
		P(2)-O(11)	1.504(9)
		P(2)-O(10)	1.517(9)
O(1)#1-U(1)-O(1)	179.998(1)	P(2)-C(10)	1.766(16)
O(3)-U(2)-O(2)	175.3(4)	P(2)-C(16)	1.768(13)
<u>Symmetry codes: #1 -x+2, -y, -z; #2 x, y, z-1; #3 -x+2, -y, -z+1; #4 -x+2, -y+1, -z; #5 x, y, z+1; #6 -x+2, -y+1, -z+1.</u>			
2		3	
U(1)-O(1)	1.753(4)	U(1)-O(2)	1.763(7)
U(1)-O(2)	1.753(4)	U(1)-O(1)	1.777(7)
U(1)-O(5)	2.299(3)	U(1)-O(4)	2.276(6)
U(1)-O(6)	2.337(3)	U(1)-O(10)#1	2.307(7)
U(1)-O(7)	2.400(3)	U(1)-O(8)#2	2.312(6)
U(1)-O(4)	2.443(3)	U(1)-O(6)#1	2.464(7)
U(1)-O(3)	2.498(3)	U(1)-O(5)#1	2.526(6)
Zn(1)-O(8)	1.925(3)	Cd(1)-O(7)#3	2.228(7)
Zn(1)-O(9)	1.935(3)	Cd(1)-N(3)#4	2.238(8)
Zn(1)-O(10)#1	1.951(3)	Cd(1)-O(3)#5	2.266(6)
Zn(1)-N(1)	1.974(4)	Cd(1)-N(1)	2.290(8)
		Cd(1)-O(9)	2.384(7)
		Cd(1)-O(5)	2.512(7)
P(1)-O(8)	1.509(3)	P(1)-O(3)	1.482(7)
P(1)-O(6)	1.516(4)	P(1)-O(4)	1.523(7)
P(1)-C(3)	1.783(5)	P(1)-C(1)	1.779(12)
P(1)-C(4)	1.795(5)	P(1)-C(7)	1.786(10)
P(2)-O(5)	1.493(4)	P(2)-O(7)	1.483(7)
P(2)-O(9)	1.500(4)	P(2)-O(8)	1.519(7)
P(2)-C(12)	1.793(5)	P(2)-C(16)	1.787(10)
P(2)-C(13)	1.793(6)	P(2)-C(10)	1.793(13)
O(1)-U(1)-O(2)	178.75(17)	O(2)-U(1)-O(1)	178.3(3)

Symmetry codes: #1 x, y+1, z for 2; #1 -x+1, -y, -z+1; #2 x, y, z-1; #3 -x, -y, -z+2; #4 x+1, y-1, z; #5 -x, -y, -z+1 for 3.

4

U(1)-O(2)	1.760(5)	U(1)-O(1)	1.742(7)
U(1)-O(1)	1.769(5)	U(1)-O(2)	1.743(7)
U(1)-O(13)#1	2.259(4)	U(1)-O(13)#1	2.277(6)
U(1)-O(3)	2.275(5)	U(1)-O(3)	2.274(6)
U(1)-O(4)	2.300(4)	U(1)-O(4)	2.277(6)
U(1)-O(5)	2.277(5)	U(1)-O(5)	2.284(6)
U(2)-O(7)	1.747(5)	U(2)-O(7)	1.744(8)
U(2)-O(8)	1.750(5)	U(2)-O(8)	1.749(7)
U(2)-O(11)#1	2.296(5)	U(2)-O(11)#1	2.266(7)
U(2)-O(9)	2.313(4)	U(2)-O(9)	2.310(6)
U(2)-O(6)#1	2.329(5)	U(2)-O(6)#1	2.326(7)
U(2)-O(15)#2	2.469(5)	U(2)-O(15)#2	2.454(8)
U(2)-O(16)#2	2.482(5)	U(2)-O(16)#2	2.504(7)
Cd(1)-O(14)	2.215(5)	Mn(1)-O(14)	2.078(7)
Cd(1)-O(10)#3	2.293(5)	Mn(1)-O(10)#3	2.161(8)
Cd(1)-O(12)	2.324(5)	Mn(1)-O(12)	2.180(7)
Cd(1)-N(3)	2.245(6)	Mn(1)-N(3)	2.184(9)
Cd(1)-N(1)	2.254(6)	Mn(1)-N(1)	2.212(9)
P(1)-O(5)	1.510(5)	P(1)-O(5)	1.515(7)
P(1)-O(6)	1.514(5)	P(1)-O(6)	1.513(7)
P(1)-C(1)	1.813(8)	P(1)-C(1)	1.771(11)
P(1)-C(7)	1.768(7)	P(1)-C(7)	1.794(9)
P(2)-O(14)	1.475(5)	P(2)-O(14)	1.480(7)
P(2)-O(3)	1.509(5)	P(2)-O(3)	1.522(6)
P(2)-C(10)	1.787(8)	P(2)-C(11)	1.771(12)
P(2)-C(16)	1.811(7)	P(2)-C(17)	1.835(15)
P(3)-O(9)	1.493(5)	P(3)-O(9)	1.501(7)
P(3)-O(4)	1.509(5)	P(3)-O(4)	1.528(7)
P(3)-C(25)	1.792(7)	P(3)-C(27)	1.780(10)
P(3)-C(19)	1.799(7)	P(3)-C(21)	1.783(11)
O(2)-U(1)-O(1)	178.2(2)	O(1)-U(1)-O(2)	178.4(3)
O(7)-U(2)-O(8)	177.3(2)	O(7)-U(2)-O(8)	177.0(4)

Symmetry codes: #1 x-1, y, z; #2 x, y+1, z; #3 x, y-1, z.

6 (Co)

U(1)-O(1)#1	1.774(6)	7 (Ni)	8 (Cu)
U(1)-O(1)	1.774(6)	1.769(5)	1.775(5)
U(1)-O(11)#2	2.256(6)	2.262(4)	2.258(4)
U(1)-O(11)#3	2.256(6)	2.262(4)	2.258(4)
U(1)-O(4)	2.279(5)	2.285(4)	2.288(5)
U(1)-O(4)#1	2.279(5)	2.285(4)	2.288(5)
U(2)-O(2)	1.769(6)	1.762(5)	1.764(5)

U(2)-O(3)	1.776(6)	1.768(5)	1.771(5)
U(2)-O(8)	2.299(6)	2.296(4)	2.305(4)
U(2)-O(10)#4	2.317(5)	2.326(4)	2.312(5)
U(2)-O(5)#5	2.322(6)	2.327(4)	2.335(4)
U(2)-O(7)	2.441(6)	2.437(5)	2.442(5)
U(2)-O(6)	2.507(5)	2.506(4)	2.507(5)
M(1)-N(1)	2.122(6)	2.075(5)	1.993(5)
M(1)-N(1)#6	2.122(6)	2.075(5)	1.993(5)
M(1)-N(3)	2.153(7)	2.121(5)	2.046(5)
M(1)-N(3)#6	2.153(7)	2.121(5)	2.046(5)
M(1)-O(1W)	2.137(6)	2.116(5)	2.502(6)
M(1)-O(1W)#6	2.137(6)	2.116(5)	2.502(6)
P(1)-O(5)	1.505(6)	1.505(4)	1.503(5)
P(1)-O(4)	1.518(5)	1.513(5)	1.522(5)
P(1)-C(7)	1.781(8)	1.780(7)	1.782(8)
P(1)-C(1)	1.803(9)	1.795(8)	1.796(8)
P(2)-O(10)	1.516(5)	1.508(4)	1.511(5)
P(2)-O(11)	1.523(6)	1.522(4)	1.520(4)
P(2)-C(16)	1.777(9)	1.782(7)	1.783(8)
P(2)-C(10)	1.795(9)	1.789(7)	1.789(7)
O(1)#1-U(1)-O(1)	180.000(1)	180.000(1)	180.0(6)
O(2)-U(2)-O(3)	178.4(3)	178.3(2)	178.1(2)
Symmetry codes: #1 -x+1, -y+1, -z+1; #2 x, y, z+1; #3 -x+1, -y+1, -z; #4 -x+1, -y, -z; #5 -x+1, -y, -z+1; #6 -x+2, -y+1, -z+1.			

Table S2 Average bond lengths of six-fold and seven-fold coordinated uranium cations in **1-8**.

	Six-fold coordinated U cations		Seven-fold coordinated U cations	
	U=O (Å)	U-O (Å)	U=O (Å)	U-O (Å)
1	1.729	2.291	1.715	2.383
2	--	--	1.753	2.396
3	--	--	1.771	2.378
4	1.765	2.278	1.749	2.378
5	1.743	2.279	1.747	2.373
6	1.775	2.268	1.773	2.378
7	1.770	2.274	1.766	2.379
8	1.776	2.273	1.768	2.381

Table S3 IR spectroscopic data for **1-8**.

	C-H (aromatic ring)/cm ⁻¹	C=C, C-N, COO / cm ⁻¹	O=U=O /cm ⁻¹	O-P-O, P-C /cm ⁻¹
1		1563, 1524, 1434, 1406, 1310	960, 930, 919, 844	1088, 1041, 742, 695
2	3057	1554, 1526, 1489, 1432, 1404, 1320	948, 918, 839	1100, 1030, 750, 690
3	3131	1590, 1519, 1444, 1404, 1312	948, 909, 856	1100, 1052, 742, 698
4	3131	1584, 1519, 1440, 1380, 1311	949, 938, 901, 856	1100, 1011, 723, 698
5	3137	1569, 1525, 1440, 1405, 1310	932, 903, 839	1057, 1022, 729, 701
6	3136	1590, 1529, 1435, 1384, 1313	934, 900, 845	1099, 1016, 743, 691
7	3136	1590, 1524, 1435, 1310	936, 904, 841	1100, 1011, 743, 692
8		1529, 1454, 1407, 1313	920, 840	1100, 1042, 770, 733, 690

Table S4 Comparison of selected single-crystal XRD and IR spectroscopic data for **1-8** using Veal's empirical law $R_{\text{U}-\text{O}}(\text{pm}) = 8120v_3^{-2/3} + 89.5$.

	v_3 (cm ⁻¹) in IR	Calculate from IR (pm)	Single XRD data (pm)
1	960, 929.7, 919	172.7, 174.7, 175.4,	169.5, 172.9, 173.3
2	948, 918	173.6, 175.5	175.3
3	948, 909, 856	173.6, 176.0, 179.6	176.3, 177.7
4	948.9, 938.4, 901	173.6, 174.2, 176.5	174.7, 175.0, 176.0, 176.9
5	932, 902.5	174.6, 176.4	174.2, 174.3, 174.4
6	934.3, 900	174.5, 176.6	176.9, 177.4, 177.6
7	936.3, 904	174.3, 176.4	176.2, 176.8, 176.9
8	919.7	175.4,	176.4, 177.1, 177.5

II. Powder X-ray diffraction patterns.

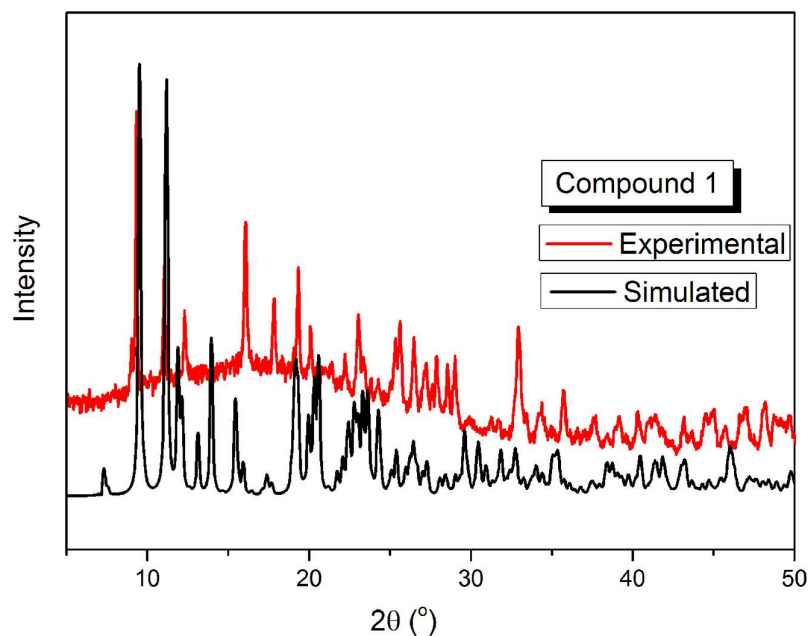


Figure S1. PXRD pattern of $\text{Co}(\text{im})_2(\text{UO}_2)_3(\text{L})_4$ **1**.

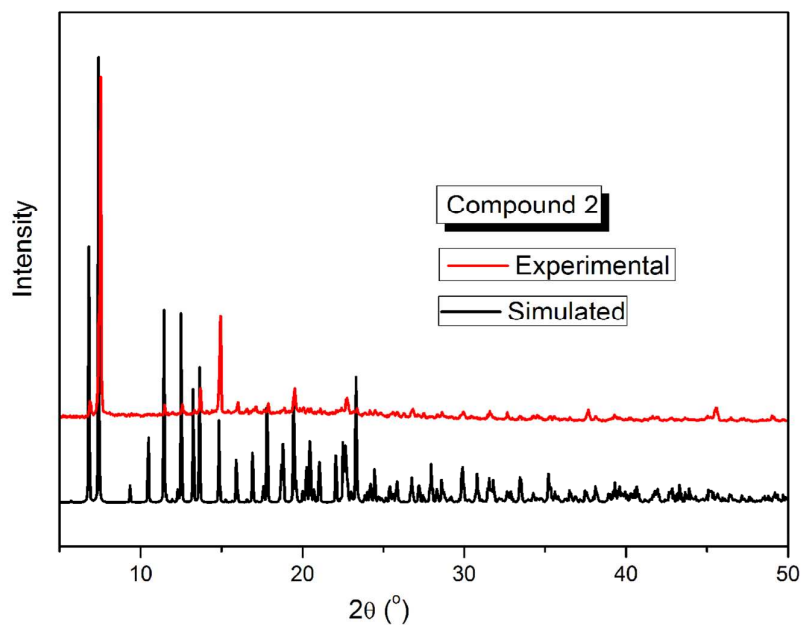


Figure S2. PXRD pattern of $\text{Zn}(\text{bpi})(\text{UO}_2)(\text{L})_2$ **2**.

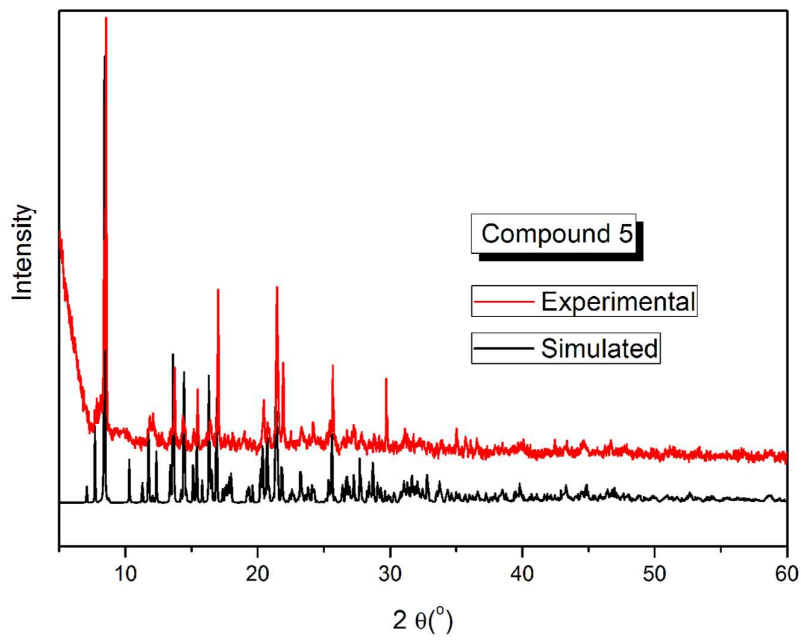


Figure S3. PXRD pattern of $\text{Mn}(\text{dib})(\text{UO}_2)_2(\text{L})_3$ **5**.

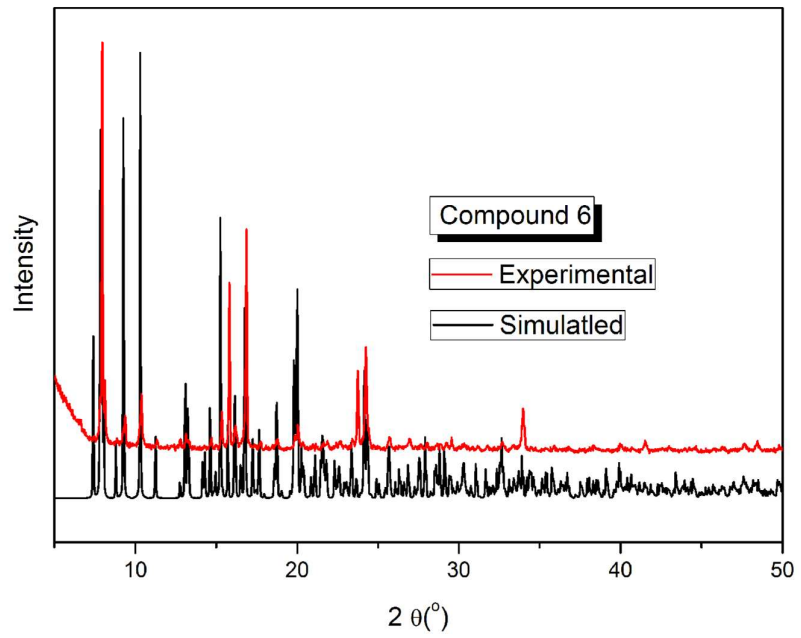


Figure S4. PXRD pattern of $[\text{Co}(\text{dib})_2(\text{H}_2\text{O})_2][(\text{UO}_2)_3(\text{L})_4] \cdot 2\text{H}_2\text{O}$ **6**.

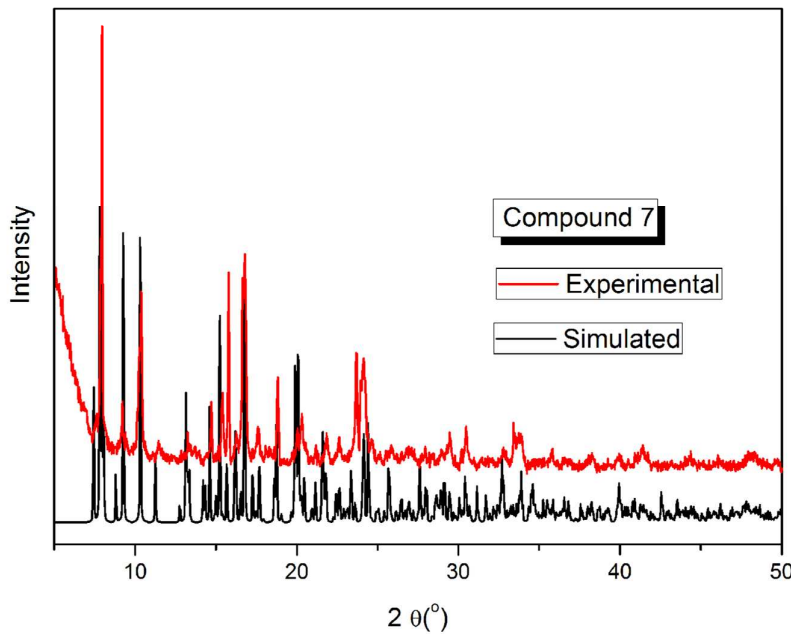


Figure S5. PXRD pattern of $[\text{Ni}(\text{dib})_2(\text{H}_2\text{O})_2][(\text{UO}_2)_3(\text{L})_4]\cdot 2\text{H}_2\text{O}$ 7.

III. Infrared spectra

The strong peaks from 960 to 900 cm^{-1} are ascribed to the antisymmetric stretching modes v_3 of uranyl dication; whilst those in the range of 839 - 812 cm^{-1} are due to the symmetric stretching vibrations v_1 . The bands in the range from 1100 to 1000 cm^{-1} and in the low wavenumber region from 750 to 690 cm^{-1} are dominated by the O-P-O bending and P-C stretching vibrations. The vibrations of the aromatic rings are indicated in the area 1590 - 1310 cm^{-1} . The peak located at 3130 cm^{-1} is attributed to the C-H stretching vibrations of the aromatic ring.

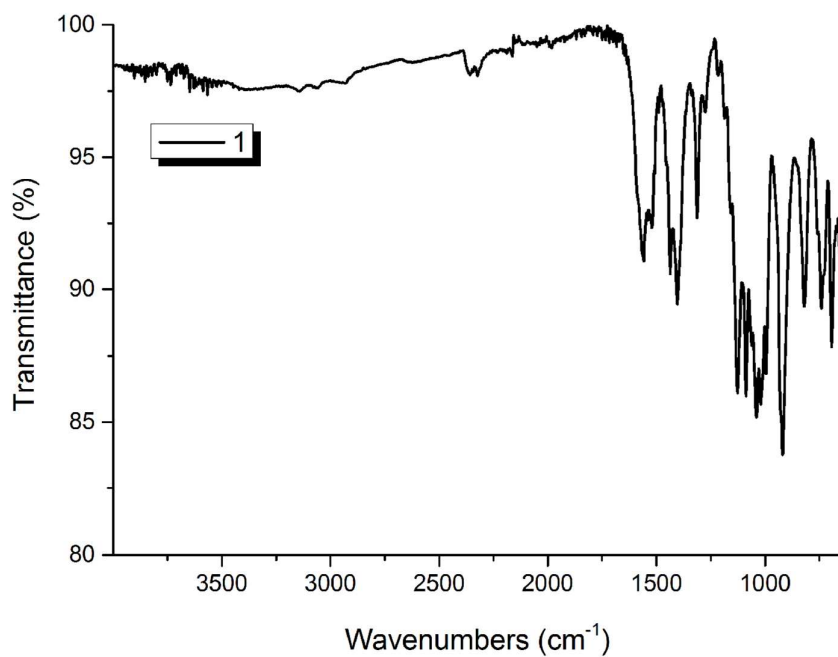


Figure S6. IR spectrum of $\text{Co}(\text{im})_2(\text{UO}_2)_3(\text{L})_4$ **1**.

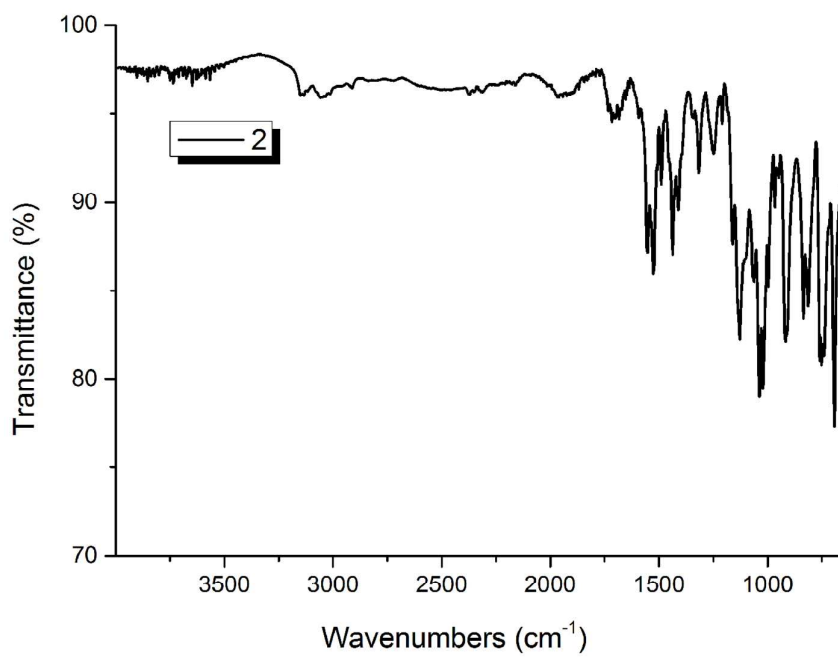


Figure S7. IR spectrum of $\text{Zn}(\text{bpi})(\text{UO}_2)(\text{L})_2$ **2**.

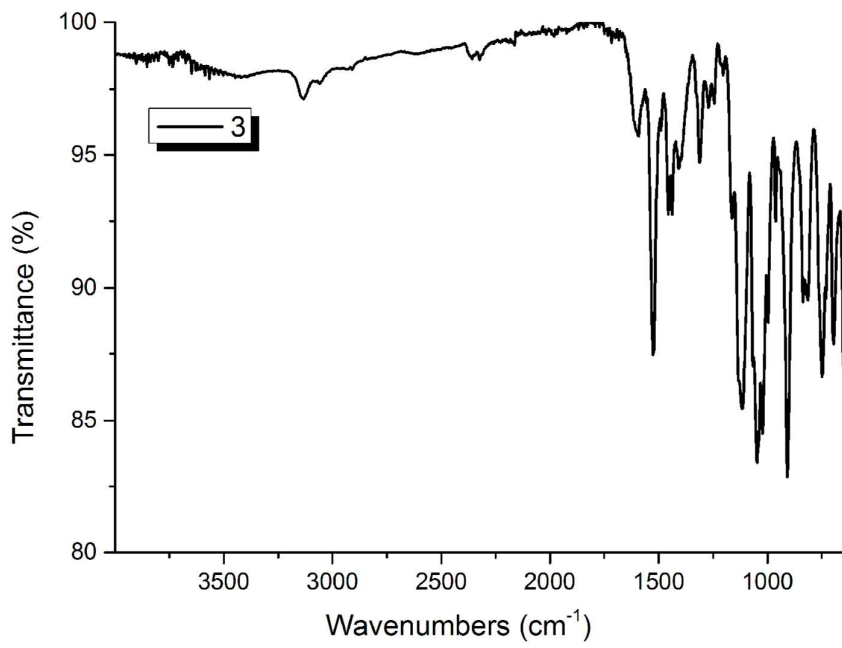


Figure S8. IR spectrum of $\text{Cd}(\text{dib})(\text{UO}_2)(\text{L})_2$ **3**.

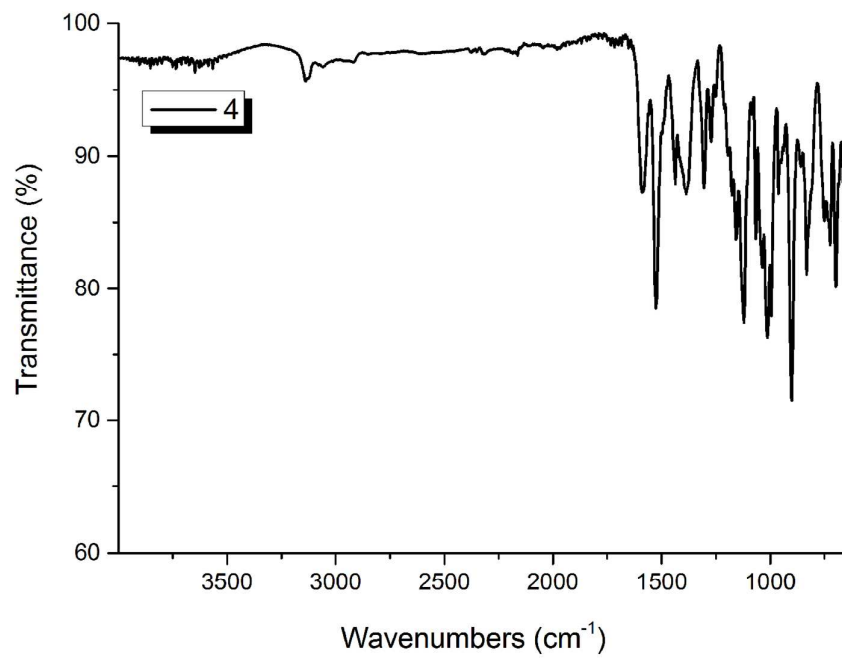


Figure S9. IR spectrum of $\text{Cd}(\text{dib})(\text{UO}_2)_2(\text{L})_3$ **4**.

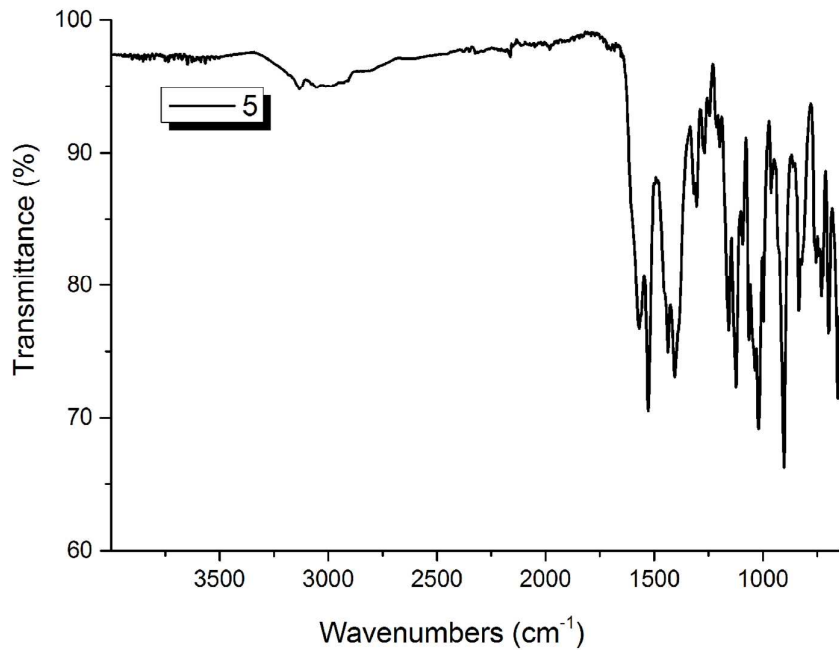


Figure S10. IR spectrum of $\text{Mn}(\text{dib})(\text{UO}_2)_2(\text{L})_3$ **5**.

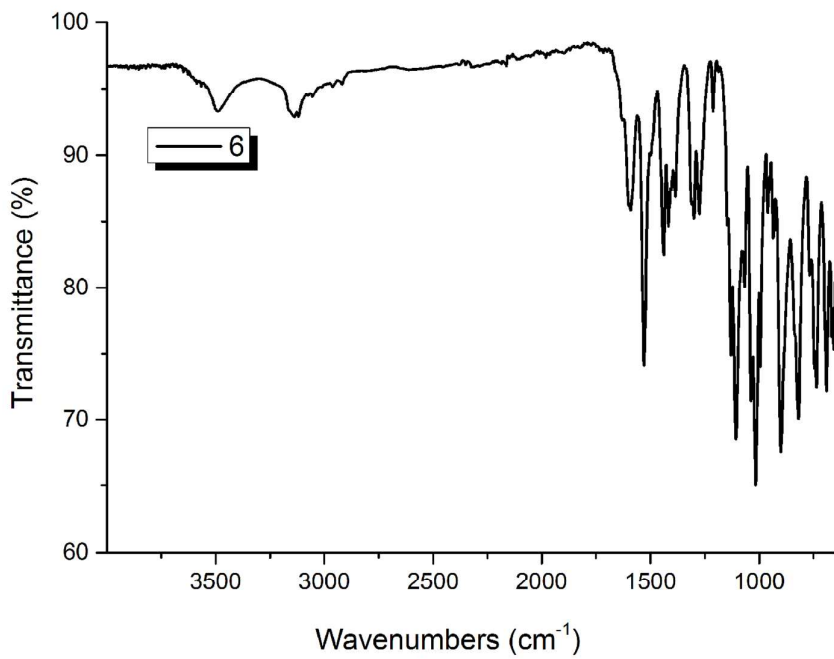


Figure S11. IR spectrum of $[\text{Co}(\text{dib})_2(\text{H}_2\text{O})_2][(\text{UO}_2)_3(\text{L})_4]\cdot 2\text{H}_2\text{O}$ **6**.

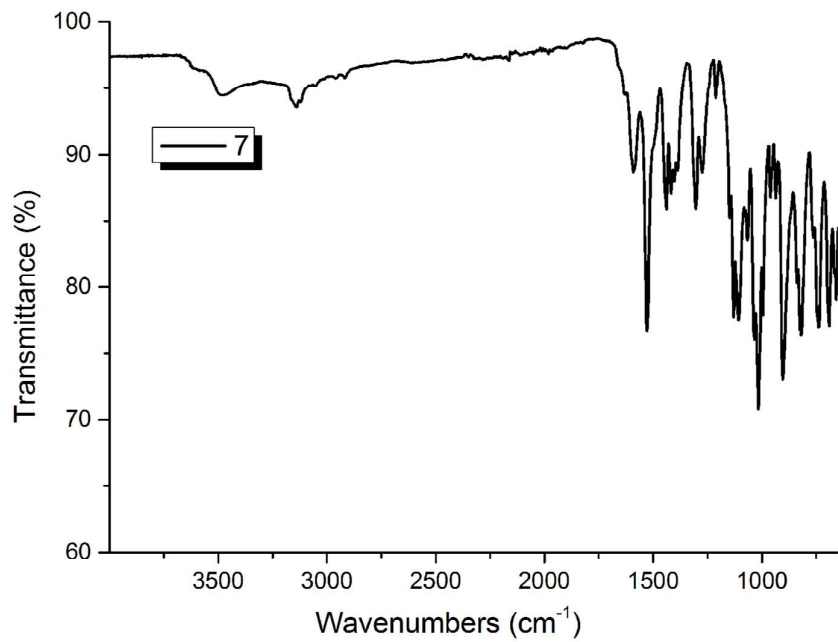


Figure S12. IR spectrum of $[\text{Ni}(\text{dib})_2(\text{H}_2\text{O})_2][(\text{UO}_2)_3(\text{L})_4]\cdot 2\text{H}_2\text{O}$ 7.

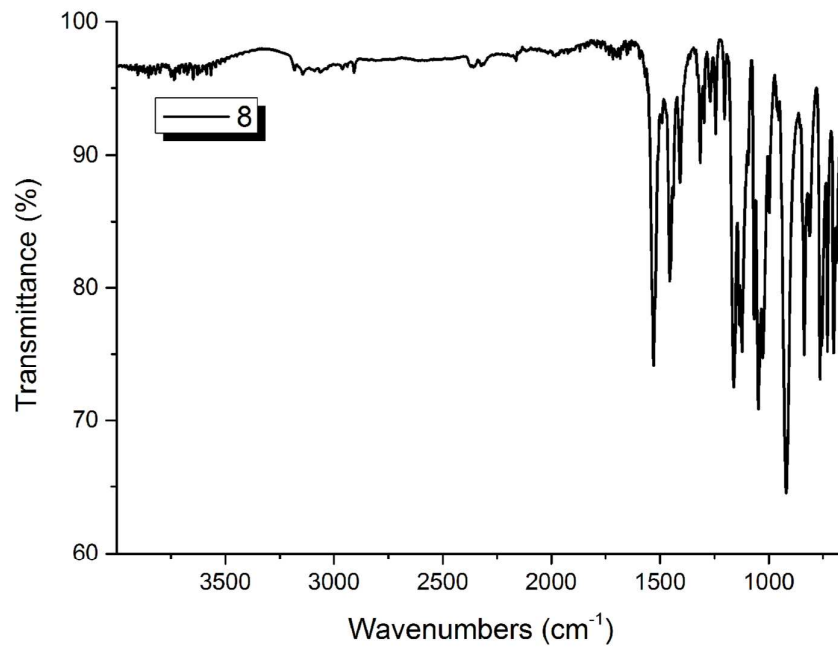


Figure S13. IR spectrum of $[\text{Cu}(\text{dib})_2(\text{H}_2\text{O})_2][(\text{UO}_2)_3(\text{L})_4]$ 8.

IV. ORTEP representation of local structures.

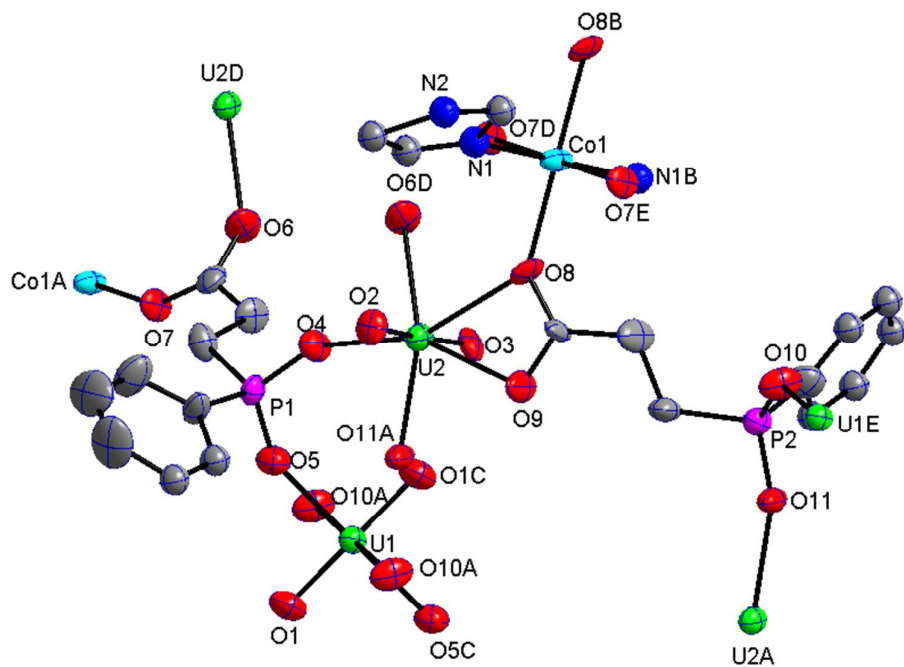


Figure S14. ORTEP representation of local structure of $\text{Co}(\text{im})_2(\text{UO}_2)_3(\text{L})_4$ **1**. Symmetry codes: A, 2-x, -y, 1-z; B, 2-x, 1-y, 1-z; C, 2-x, -y, -z; D, 2-x, 1-y, -z; E, x, y, 1+z.

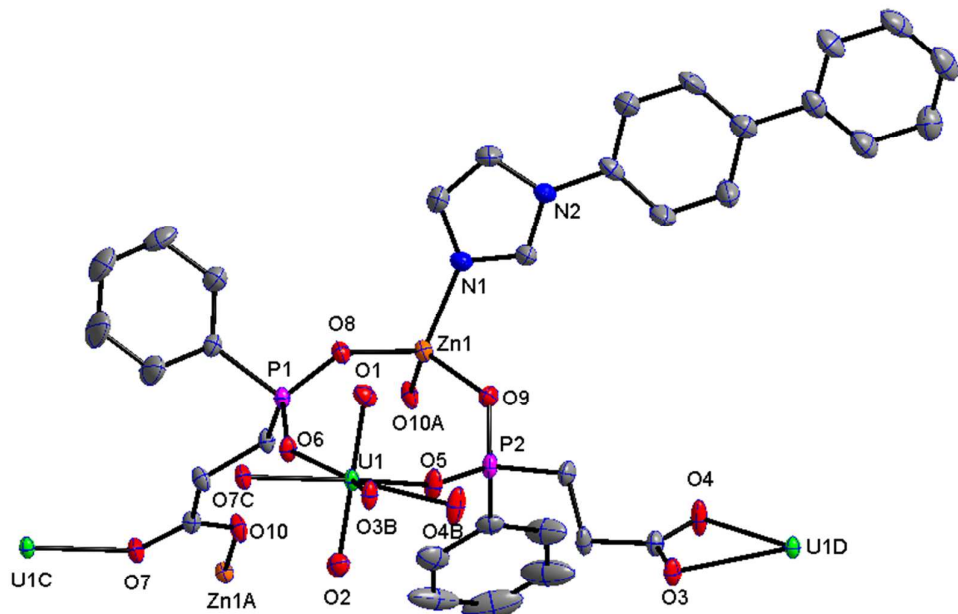


Figure S15. ORTEP representation of local structure of $\text{Zn}(\text{bpi})(\text{UO}_2)(\text{L})_2$ **2**. Symmetry codes: A, 1-x, 2-y, 1-z; B, 1-x, 0.5+y, 1.5-z; C, 1-x, 3-y, 1-z; D, 1-x, -0.5+y, 1.5-z.

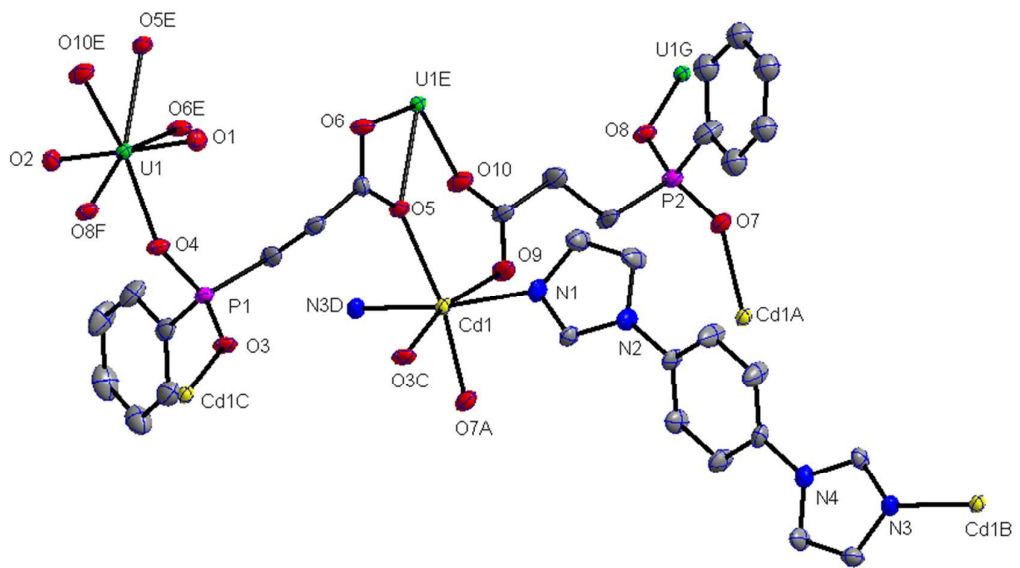


Figure S16. ORTEP representation of local structure of $\text{Cd}(\text{dib})(\text{UO}_2)(\text{L})_2$ **3**. Symmetry codes: A, $-x, -y, 2-z$; B, $-1+x, 1+y, z$; C, $-x, -y, 1-z$; D, $1+x, -1+y, z$; E, $1-x, -y, 1-z$; F, $x, y, -1+z$; G, $x, y, 1+z$.

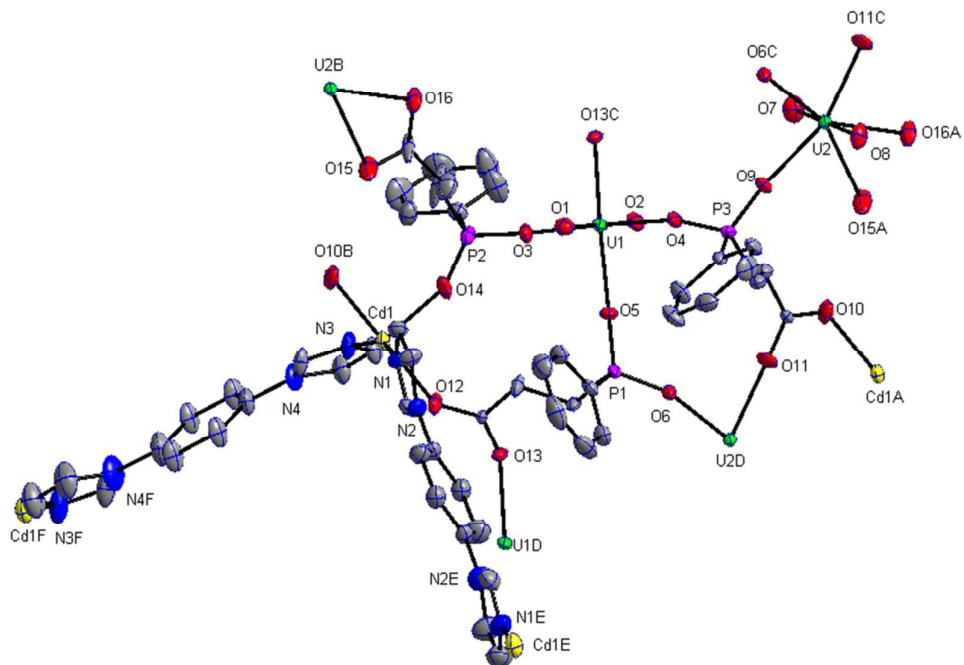


Figure S17. ORTEP representation of local structure of $\text{Cd}(\text{dib})(\text{UO}_2)_2(\text{L})_3$ **4**. Symmetry codes: A, $x, 1+y, z$; B, $x, -1+y, z$; C, $-1+x, y, z$; D, $1+x, y, z$; E, $2-x, -y, 1-z$; F, $2-x, -1-y, -z$.

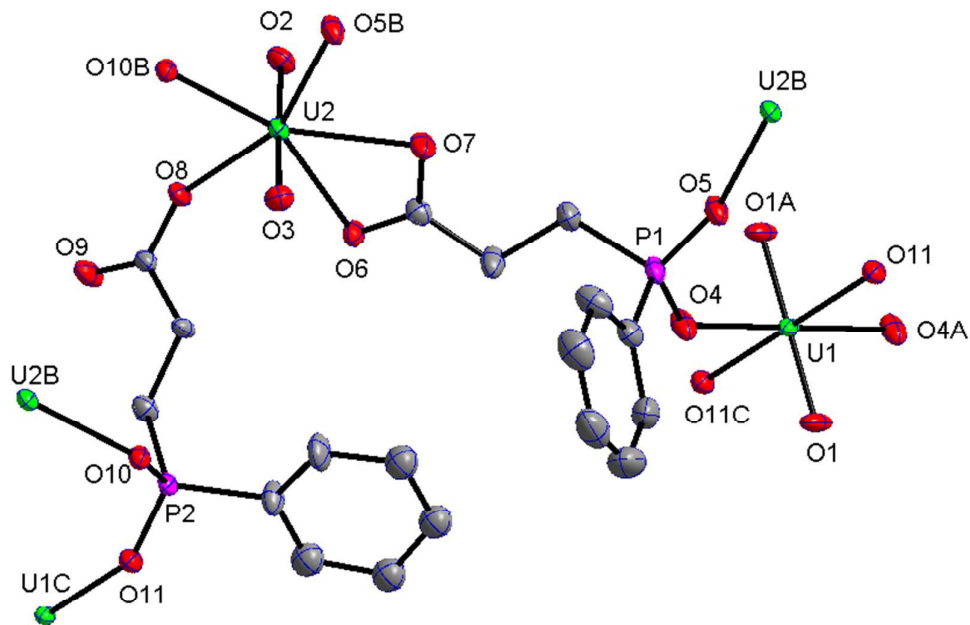


Figure S18. ORTEP representation of local structure of $[\text{Co}(\text{dib})_2(\text{H}_2\text{O})_2][(\text{UO}_2)_3(\text{L})_4]\cdot 2\text{H}_2\text{O}$ **6**. Symmetry codes: A, $1-x$, $1-y$, $1-z$; B, $1-x$, $-y$, $1-z$; C, x , y , $-1+z$.

V. Excitation and Emission spectra.

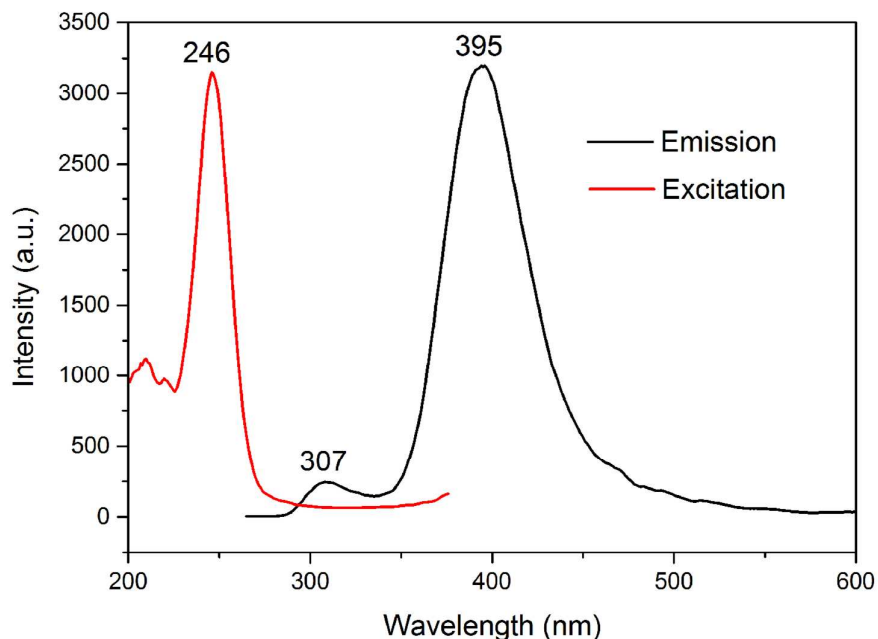


Figure S19. Excitation and emission spectra of $\text{Co}(\text{im})_2(\text{UO}_2)_3(\text{L})_4$ **1**.

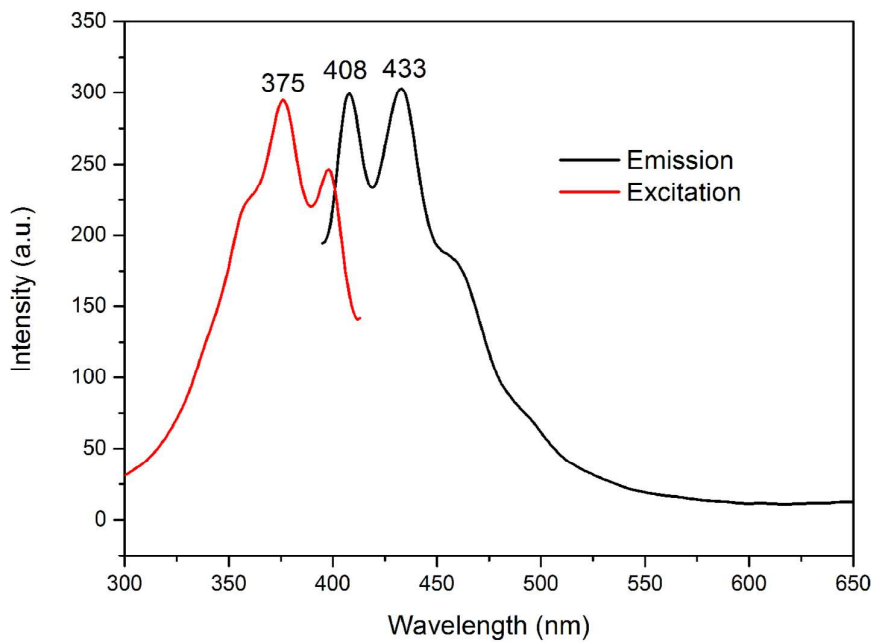


Figure S20. Excitation and emission spectra of $\text{Mn}(\text{dib})(\text{UO}_2)_2(\text{L})_3$ **5**.

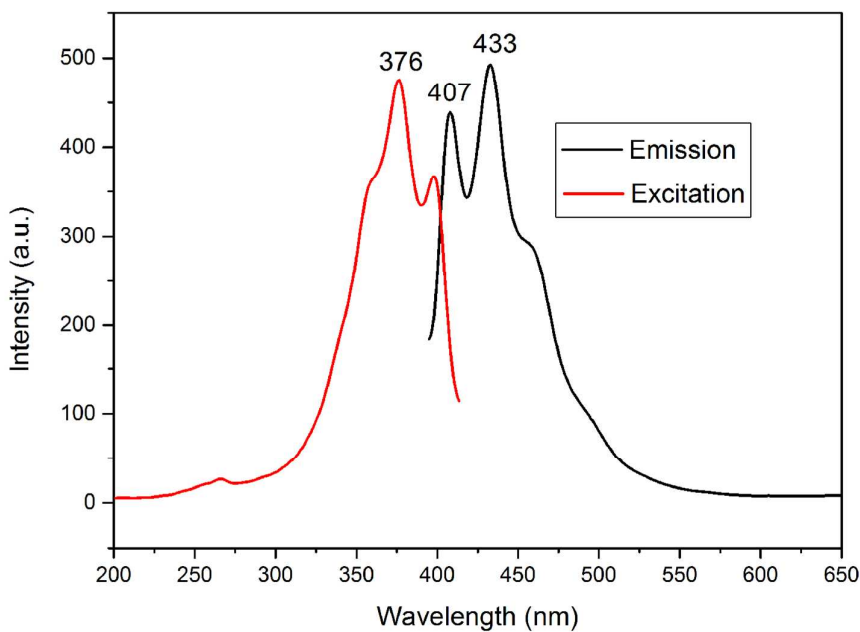


Figure S21. Excitation and emission spectra of $[\text{Co}(\text{dib})_2(\text{H}_2\text{O})_2][(\text{UO}_2)_3(\text{L})_4]\cdot 2\text{H}_2\text{O}$ **6**.

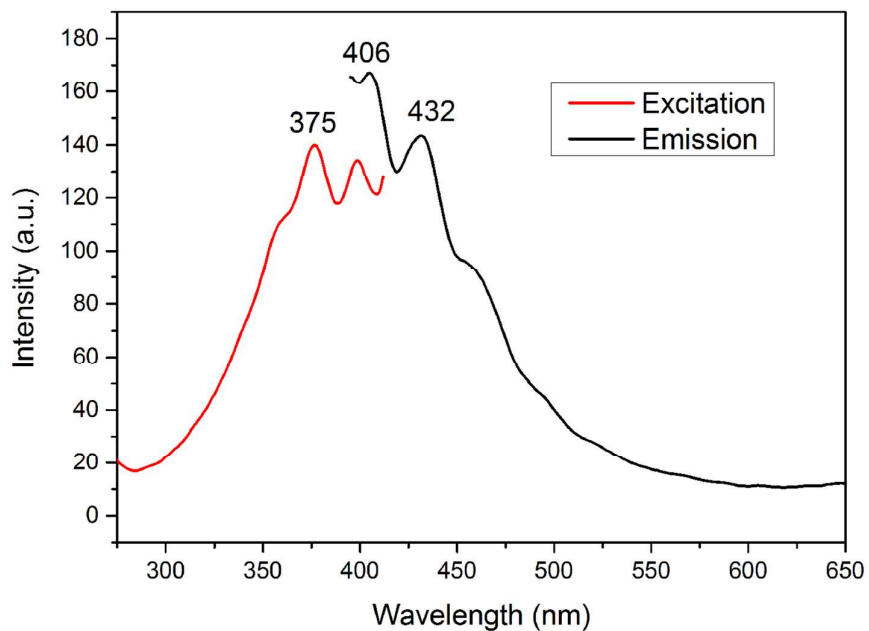


Figure S22. Excitation and emission spectra of $[\text{Ni}(\text{dib})_2(\text{H}_2\text{O})_2][(\text{UO}_2)_3(\text{L})_4] \cdot 2\text{H}_2\text{O}$
7.

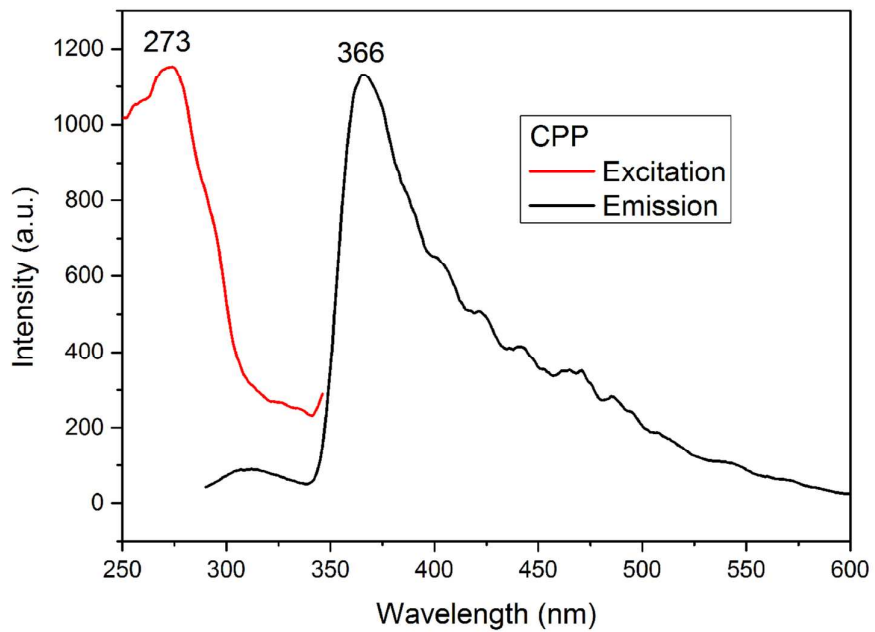


Figure S23. Excitation and emission spectra of the carboxphosphinate ligand **CPP**.

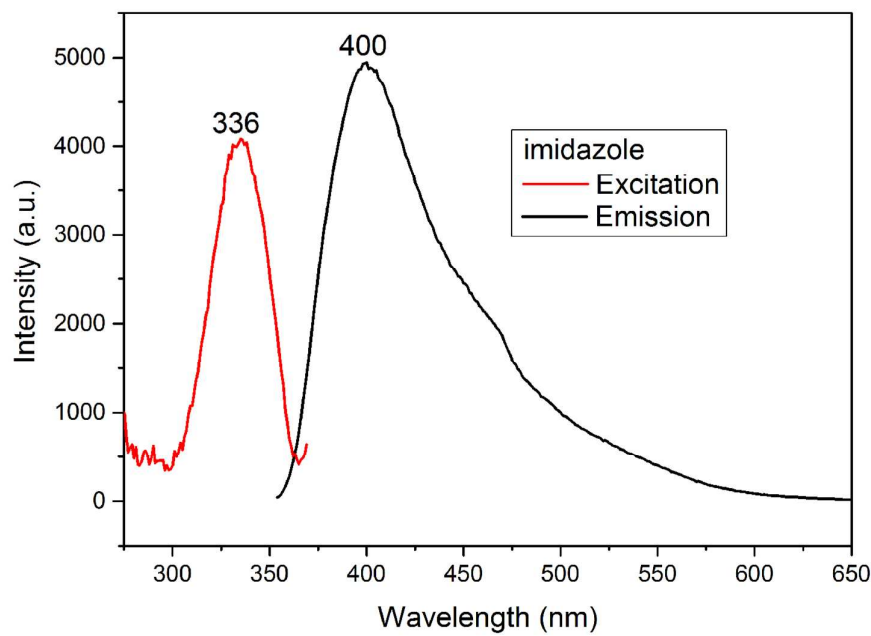


Figure S24. Excitation and emission spectra of imidazole.

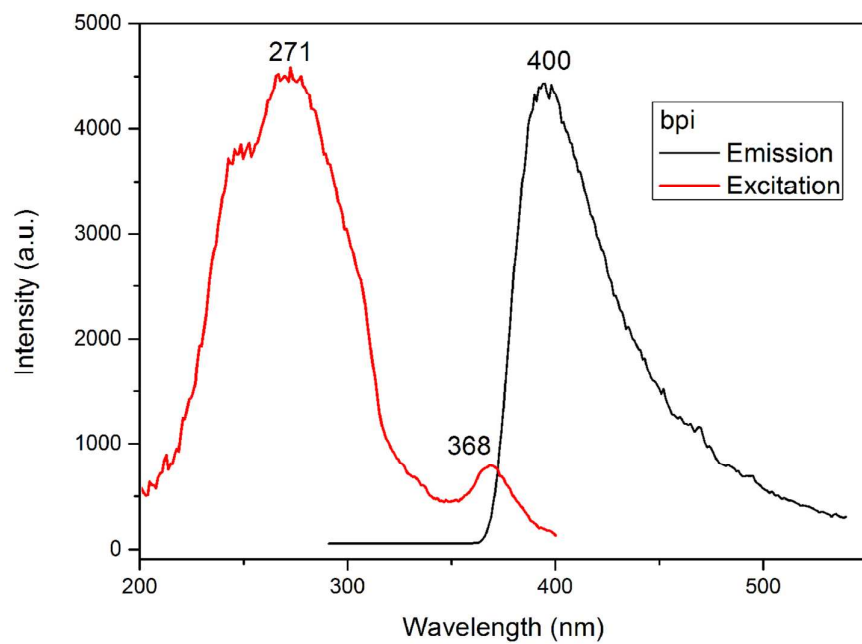


Figure S25. Excitation and emission spectra of **bpi**.

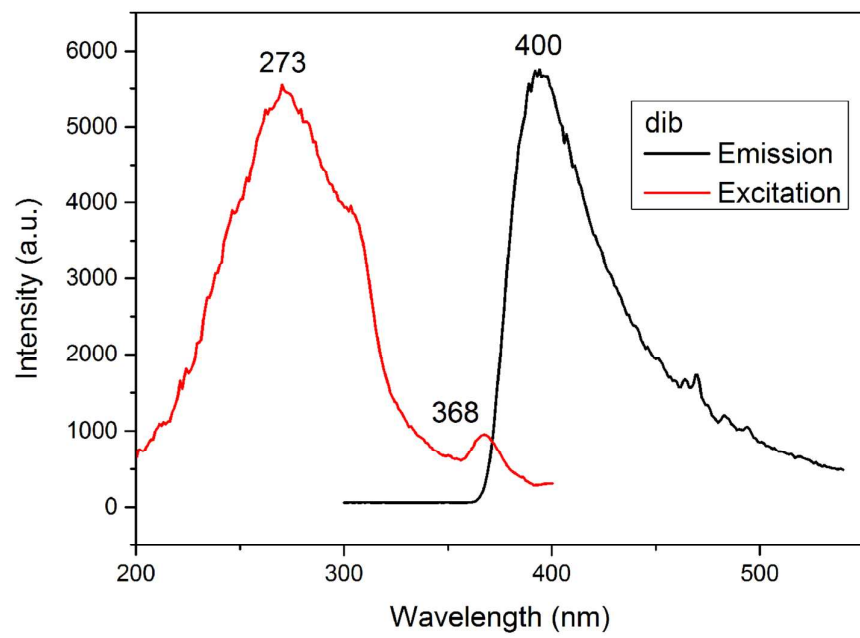


Figure S26. Excitation and emission spectra of **dib**.